THE JOURNAL OF PHYSICAL CHEMISTRY B

ARTICLE

pubs.acs.org/JPCB

Electron Transfer Mechanism of Cytochrome *c* at the Oil/Water Interface as a Biomembrane Model

Yoko Imai, Takayasu Sugihara,† and Toshiyuki Osakai*

Department of Chemistry, Graduate School of Science, Kobe University, Nada, Kobe 657-8501, Japan

ABSTRACT: The electron transfer (ET) between cytochrome *c* (Cyt *c*) in water (W) and 1,1′-dimethylferrocene (DiMFc) in 1,2-dichloroethane (DCE) was studied. The cyclic voltammograms obtained for the interfacial ET under various conditions could be well reproduced by digital simulation based on the ion-transfer (IT) mechanism, in which the ET process occurs not at the DCE/W interface but in the W phase nearest the interface. In this mechanism, the current signal is due to the IT of $DiMFc^+$ as the reaction product. On the other hand, the measurement of the double-layer capacity showed that Cyt *c* is adsorbed at the DCE/W interface. However, the contribution from the adsorbed proteins to the overall ET is considered to be small because of the thicker reaction layer in the IT mechanism. These findings would offer a useful suggestion for the behaviors of Cyt *c* in vivo.

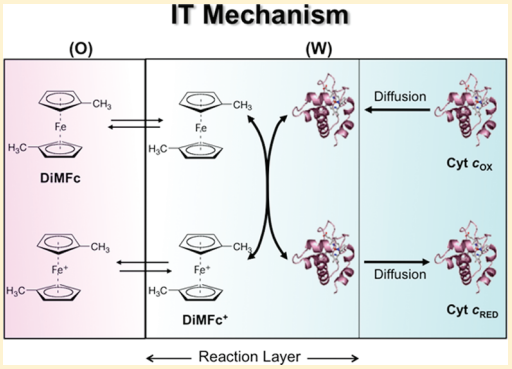

INTRODUCTION

A heme protein, cytochrome *c* (Cyt *c*), is one of the most extensively studied redox proteins. In the mitochondrial respiratory chain, Cyt *c* transports an electron from Cyt *c* reductase (complex III) to Cyt *c* oxidase (complex IV).[1] However, the detailed electron-transfer (ET) mechanism in vivo remains to be clarified.

It is not necessarily easy to achieve direct ET reaction of Cyt *c* at solid electrode surfaces since the heme iron center is buried beneath the surface of the protein. This difficulty has been overcome by modifying electrode surfaces with metal oxides,[2] adatoms,[3] gold nanoparticles,[4] carbon nanotubes,[5,6] graphene,[7] etc. The modification with such nanomaterials facilitates interaction between the heme center and the underlying electrode. From a similar point of view, rough hydrophilic electrode surfaces such as edge-plane pyrolytic graphite[8] have been applied to achieve fast ET reactions for redox proteins including Cyt *c*.

In this study, we have employed an interface between two immiscible electrolyte solutions (ITIES), the so-called organic solvent or oil/water (O/W) interface, to study the interfacial ET of Cyt *c*. The polarized O/W interface is the simplest and good model of a biomembrane.[9] Unlike biomembrane models such as phospholipid bilayer membranes, liquid membranes, and liposomes, the O/W interface comprises only one interface whose Galvani potential difference can be controlled electrochemically; thus, a rigorous thermodynamic and kinetic analysis can be done for the charge (ion and/or electron) transfer occurring at the O/W interface.[9−14]

At a polarized O/W interface, we may observe an ET reaction between a hydrophilic redox couple (O1/R1) in W and a hydrophobic redox couple (O2/R2) in O by means of voltammetric techniques under appropriate conditions.[15]

$$O1(W) + R2(O) \rightleftharpoons R1(W) + O2(O)$$

The first example was reported by Samec et al.,[16] who used cyclic voltammetry to obtain a well-defined wave for the ET between ferrocene (Fc) in nitrobenzene (NB) and $Fe(CN)_6^{3-}$ in W. In our previous study,[17] however, a digital simulation analysis of cyclic voltammograms showed that the observed current was not due to heterogeneous ET at the O/W interface but due to the ion transfer (IT) of the ferrocenium cation (Fc^+) that was generated by a homogeneous ET reaction of Fc being partially distributed to the W phase. This IT mechanism has been confirmed and studied in detail by Tatsumi et al.[18−20] A similar IT mechanism was also reported for the ET reaction between L-ascorbic acid (W) and chloranil (O).[21−23] On the other hand, "true" or heterogeneous ET at the O/W interface can be realized by using as the redox species in O extremely hydrophobic compounds such as metal complexes of biphthalocyanine[24,25] and 5,10,15,20-tetraphenylporphyrin.[26,27]

In recent years, there has been increased attention to ET reactions of redox enzymes or proteins at the O/W interface. Georganopoulou et al.[28] first reported an interfacial ET reaction between β-D-glucose in W and the 1,1′-dimethylferrocenium ion ($DiMFc^+$) in O being catalyzed by glucose oxidase (GOD). Sugihara et al.[29] examined the reaction mechanism using digital simulation of cyclic voltammograms, concluding that the observed current signal was due to the IT of $DiMFc^+$ from O to W, which induced the enzymatic oxidation of glucose in the W phase. In view of realizing a heterogeneous ET mediated by an enzyme at the O/W interface, we have recently employed a membrane-bound enzyme, D-fructose dehydrogenase (FDH), to study the interfacial ET with $DiMFc^+$ (electron acceptor) in O. However, it

Received: September 26, 2011
Revised: December 11, 2011
Published: December 13, 2011

ACS Publications © 2011 American Chemical Society

dx.doi.org/10.1021/jp2092658 | *J. Phys. Chem. B* 2012, 116, 585–592

Scheme 1. Schematic Representation of the Electrochemical Cell[a]

I	II	III	IV	
Ag | AgCl (RE1)	4 mM TPnACl 20 mM $MgSO_4$ (W)	*y* M DiMFc 0.02 M BTPPATClPB (DCE)	*x* mM Cyt *c* 0.1 M LiCl (W)	0.1 M LiCl (W)	AgCl | Ag (RE2)

[a] $x = 0.2-0.8$ and $y = 0.01-0.04$.

has been suggested that the heme c site of FDH adsorbed at the O/W interface, i.e., the active site to bind the electron acceptor, is located in the W-phase side of the interface.[30]

In this study, we have focused on the ET reaction of Cyt *c* at a polarized 1,2-dichloroethane (DCE)/W interface, which was previously observed by Dryfe et al.[31] They reported a clear voltammetric wave for the ET reaction of Cyt *c* (W) with DiMFc (O); however, the detailed reaction mechanism is still unclear. Here we applied the previously developed digital simulation technique[17] to clarify the reaction mechanism.

EXPERIMENTAL SECTION

Reagents. Cyt *c* (from horse heart; ≥96%) was supplied from Sigma predominantly in the oxidized form[32] and used without further purification. The supporting electrolyte for the DCE phase, bis(triphenylphosphoranylidene)ammonium tetrakis(chlorophenyl)borate (BTPPATClPB), was prepared and purified as reported previously.[33] DiMFc (Tokyo Chemical Industry, Japan) was recrystallized from methanol, but a preliminary voltammetric measurement revealed that the oxidized species ($DiMFc^+$) was still contained as an ionic impurity in the recrystallized salt of DiMFc; to remove this, the DCE-phase solution containing DiMFc and BTPPATClPB was washed in advance with the same volume of an aqueous solution of 3.5×10^{-5} M (=mol dm^{-3}) $BTPPA^+Cl^-$ (Aldrich). Tetrapentylammonium chloride (TPnACl; Tokyo Chemical Industry) and DCE (for HPLC; Wako Pure Chemical Industries, Japan) were used without further purification. All other reagents were of the highest grade available and used as received.

Electrochemical Measurements. Cyclic voltammetry (CV), potential-step chronoamperometry (PSCA), and ac voltammetry were performed using a four-electrode electrolytic cell.[34] Unless noted otherwise, the electrochemical cell is shown in Scheme 1.

Here, RE1 and RE2 are the reference electrodes, and the double bar represents the polarized DCE/W interface (surface area $A = 0.071$ cm^2). The pH of the W phase (III) was adjusted to 6.9 with a $Na_2HPO_4-NaH_2PO_4$ buffer (the phosphate concentration being 4 mM in the W phase). A platinum coil electrode and a Ag/AgCl electrode were immersed into the O and W phases, respectively, and used as the counter electrodes. The interface between phases I and II was formed in a Luggin capillary. Although the respective phases contained no common ion, the Galvani potential difference was found to be practically time independent at least for several hours after preparation of the reference electrode. The reproducibility of the electrode potential was also good (±5 mV). The interface between phases III and IV was formed by means of glass sinter. In this study, neither the W nor DCE phase was deoxygenated. All electrochemical measurements were carried out at room temperature (23−27 °C). For further details of the electrolytic cell, see the previous paper.[34]

The voltammetric measurements were performed using a previously developed computer assisted system.[34] The test DCE/W interface was polarized by using a four-electrode potentiostat[34] (HA1010 mM1A, Hokuto Denko, Japan). The solution resistance was compensated for by means of a positive feedback circuit attached to the potentiostat. A low-pass filter mounted in the potentiostat was appropriately used to reduce noise in the current signal. The potential E applied to the electrolytic cell is related to the Galvani potential difference, $\Delta_O^W\phi$ ($\equiv\phi^W - \phi^O$), across the O/W interface as

$$E = \Delta_O^W\phi + \Delta E_{ref} \quad (1)$$

where ΔE_{ref} is the constant determined only by the reference electrodes used. The value of ΔE_{ref} was estimated by referring to the reversible half-wave potential, i.e., the midpoint potential in CV (+0.463 V) for the transfer of the tetramethylammonium ion (TMA^+)

$$E^r_{1/2,j} = \Delta_O^W\phi_j^o + \frac{RT}{F}\ln\frac{\gamma_j^O\sqrt{D_j^W}}{\gamma_j^W\sqrt{D_j^O}} + \Delta E_{ref} \quad (2)$$

Here, $\Delta_O^W\phi_j^o$ is the standard ion-transfer potential of ion j ($\Delta_O^W\phi_j^o$ = +0.160 V[35] for $j = TMA^+$); γ_j^α and D_j^α are its activity coefficient and diffusion coefficient in phase α (=O or W), respectively; and R, T, and F have their usual meanings. By assuming $\gamma_j^O/\gamma_j^W = 1$ and $D_j^W/D_j^O = 0.875$ (being approximated to the reciprocal ratio of the viscosities of W and DCE; see below), the value of ΔE_{ref} was estimated to be +0.305 V.

In ac voltammetry,[36] a small ac voltage (10 mV rms; frequency $f = 6$ Hz) was superimposed on a dc sweep voltage (5 mV s^{-1}). From the ac current signal detected by the potentiostat, the real (Y') and imaginary (Y'') parts of the admittance of the test O/W interface were recorded by means of a two-phase lock-in amplifier (LI 5640, NF, Japan). The double-layer capacity (C_{dl}) of the interface was evaluated from Y'' as $C_{dl} = Y''/(2\pi fA)$.

To determine the formal potential of the interfacial ET reaction studied, a voltammetric measurement was performed with an electron conductor separating oil−water (ECSOW) system.[17,37] In this system the electron conductor (EC) phase was inserted between the DCE and W phases. The phase compositions and the reference electrodes used were almost the same as those in Scheme 1. By referring to a previous paper,[38] however, the supporting electrolyte in phase III was changed from 0.1 M LiCl to 0.1 M $NaClO_4$ for ensuring an ideal electrode reaction of Cyt *c*. The EC phase was composed of Pt and Au disk electrodes (each area, 0.071 cm^2) being connected by an electric wire; the Pt and Au electrodes were immersed in the DCE and W phases, respectively. Prior to each measurement, the Pt and Au electrodes were freshly polished with 0.25 μm diamond slurry and rinsed with purified water. In this study, according to the previous paper,[38] the electrode reaction of Cyt *c* was developed at the Au electrode in the W phase containing 10 mM 4,4′-bipyridine as an electron mediator.

Distribution Experiment. The DCE−W partition coefficient of DiMFc was determined by solvent extraction as follows: DiMFc was initially added to 20 mL of DCE so that the concentration became 0.05, 0.1, and 0.2 M. To remove $DiMFc^+$ as an ionic impurity, the DCE solution was washed with the same volume of a 3.5×10^{-5} M $BTPPA^+Cl^-$ aqueous solution. The

dx.doi.org/10.1021/jp2092658 | J. Phys. Chem. B 2012, 116, 585–592

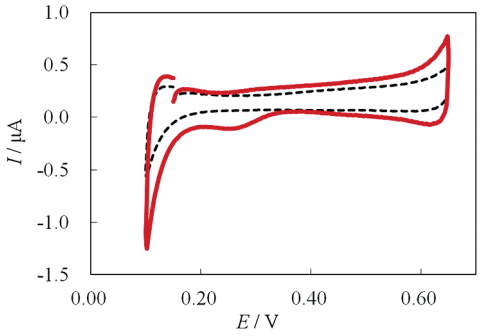

Figure 1. Cyclic voltammogram recorded using the electrochemical cell (Scheme 1) with $x = 0.4$ and $y = 0.02$. The dashed line represents the base current obtained in the absence of Cyt *c* in W. Scan rate: 50 mV s^{-1}.

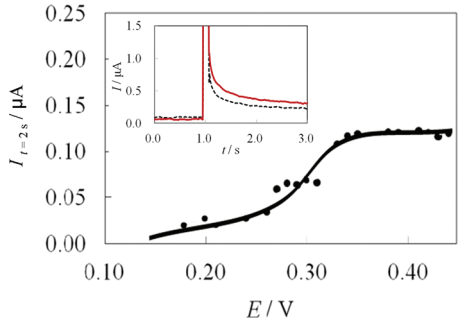

Figure 2. Current−potential curve obtained by PSCA using the electrochemical cell (Scheme 1) with $x = 0.4$ and $y = 0.02$. The inset shows a representative chronoamperogram obtained for a potential step from 0.180 to 0.450 V. The dashed line shows the base current obtained in the absence of Cyt *c*. The current sampled at $t = 2$ s, corrected for the base current, was used for obtaining the current−potential curve.

DCE solution was then equilibrated with 70 mL of W by standing overnight at 25 ± 0.1 °C. The DiMFc partially distributed to the W phase was back-extracted into 20 mL of *n*-hexane. Almost the whole solvent was evaporated using a rotary evaporator; to the resultant condensed DiMFc solution was then added 3 mL of DCE. Finally, the concentration of DiMFc in DCE was determined spectrophotometrically (molar absorption coefficient: $\varepsilon = 9790\ M^{-1}\ cm^{-1}$ at 223 nm).

Digital Simulation. Calculations of cyclic voltammograms and potential-step chronoamperograms were performed by a normal explicit finite difference (FED) digital simulation technique[39,40] with an exponentially expanding space grid method.[40,41] Spreadsheet programs for the calculations were written in Microsoft Excel 2007 and used for manual curve-fitting analyses. For further details, see the previous paper.[17]

RESULTS AND DISCUSSION

CV. In Figure 1, solid and dashed lines show the cyclic voltammograms, respectively, in the presence and absence of 0.4 mM Cyt *c* in the W phase. As reported by Dryfe et al.,[31] a small but clear wave due to the ET between Cyt *c* and DiMFc is observed at around 0.3 V. However, the anodic (positive current) wave shows a plateau but no peak. The anodic current measured at 0.35 V, corrected for the base current, is increased with the square root of voltage scan rate (v), but only slightly in the higher range (>100 mV s^{-1}; data not shown). These features of the

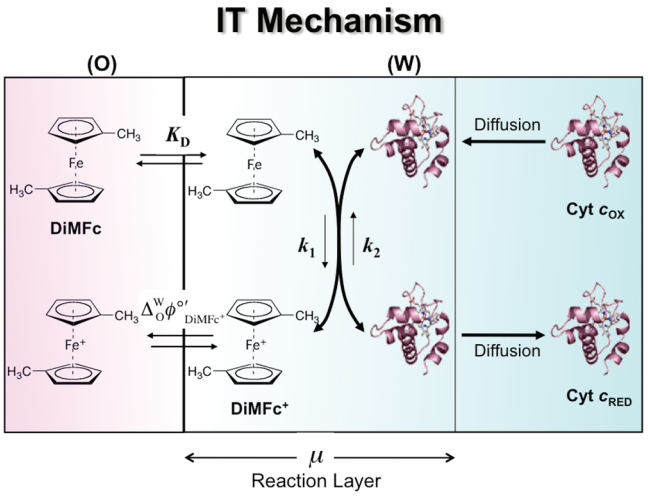

Figure 3. IT mechanism. For further details, see the text.

voltammograms are similar to those reported for the Fc(NB)−$Fe(CN)_6^{3-}$ (W) system,[16,17] suggesting that the ET reaction is not a simple heterogeneous ET but is due to an analogous IT mechanism.

In Figure 1, a current increase is also observed in the anodic final rise in the presence of Cyt *c* in W. Since its appearance is independent of the addition of DiMFc, the current increase is considered to be due to the facilitated transfer of the supporting electrolyte anion ($TClPB^-$) by the positively charged protein Cyt *c*.[42] Also in the cathodic (negative current) final descent, a relatively large current increase is observed by the addition of Cyt *c*, which might be due to the transfer of ionic impurities contained in the Cyt *c* reagent (possibly, the dodecylsulfate ion is often used as a stabilizing agent for proteins).

PSCA. Furthermore, we performed PSCA measurements, in which the potential *E* was stepped from 0.150 V to various potentials ranging from 0.180 to 0.450 V. A representative current−time (I−t) curve is shown in the inset of Figure 2. The dashed line shows the base current obtained in the absence of Cyt *c*, which is due to the charging of the O/W interface as well as the IT of supporting electrolytes and/or impurities. The charging current appears to be reduced rapidly within 0.5 s or so. The current sampled at $t = 2$ s has been corrected for the base current and plotted against different step potentials in Figure 2. The limiting current has been determined to be 0.12 μA. It should be noted that the observed limiting current is about one tenth of the diffusion-limiting current (1.24 μA) calculated by the Cottrell equation[43]

$$I(t)_{\mathrm{diff}} = nFAc^*\sqrt{\frac{D_{\mathrm{Cyt}\ c}}{\pi t}} \qquad (3)$$

where n is the number of electrons involved in the ET reaction (here $n = 1$); c^* is the bulk concentration of Cyt *c* in W; and $D_{\mathrm{Cyt}\ c}$ is the diffusion coefficient of Cyt *c* in W (here we employed a literature value[44] of $1.28 \times 10^{-6}\ cm^2\ s^{-1}$). This result suggests that the observed current is limited not by diffusion but by a slower chemical event.

Digital Simulation in CV. On the basis of the results in CV and PSCA, we propose the IT mechanism shown in Figure 3. In this mechanism, DiMFc in the O phase is partially distributed to the W phase, where Cyt *c* (in the oxidized form) diffuses from the

dx.doi.org/10.1021/jp2092658 |J. Phys. Chem. B 2012, 116, 585–592

bulk to the interface and then undergoes a homogeneous ET reaction with DiMFc. The resultant $DiMFc^+$ ion is then transferred from W to O according to the $\Delta_O^W\phi$ of the O/W interface. This IT process is responsible for the faradaic current observed experimentally. Thus, the IT mechanism involves the following elementary reactions occurring at the O/W interface or its vicinity

$$DiMFc(O) \rightleftharpoons DiMFc(W) \tag{4a}$$

$$DiMFc(W) + Cyt\ c_{OX}(W) \rightleftharpoons DiMFc^+(W) + Cyt\ c_{RED}(W) \tag{4b}$$

$$DiMFc^+(W) \rightleftharpoons DiMFc^+(O) \tag{4c}$$

where Cyt c_{OX} and Cyt c_{RED} stand for the oxidized and reduced forms of Cyt *c*, respectively.

To confirm the validity of the IT mechanism, we have performed a digital simulation analysis of cyclic voltammograms. In the analysis, the distribution of DiMFc at the O/W interface is assumed to be always in equilibrium, i.e.

$$\frac{[DiMFc]_O}{[DiMFc]_W} = K_D \tag{5}$$

where $[X]_O$ and $[X]_W$ are the concentrations of species X (=DiMFc) in O and W, respectively. Note that the relation of eq 5 holds only at the O/W interface. In the present experiments, DiMFc has been added to O in an excess amount over 0.01 M; therefore, $[DiMFc]_O$ at the interface is assumed to be equal to that in the bulk. It is also reasonably assumed that $[DiMFc]_W$ can be kept constant at the interface during voltammetric measurements, provided that the distribution equilibrium is always established. This condition seems to be satisfied for the present, totally slow ET process. In this study, the value of K_D was determined to be 6800 by solvent extraction. This value has been employed for the simulation analysis described below.

The diffusion coefficients of DiMFc, $DiMFc^+$, and Cyt *c*, used for the simulation, have been determined or estimated as described below: The diffusion coefficient of DiMFc in DCE has been determined to be 1.1×10^{-5} $cm^2\ s^{-1}$ from the reversible wave obtained by conventional CV with a Pt disk electrode, and the diffusion coefficient of $DiMFc^+$ in DCE is assumed to be identical to that of DiMFc. The diffusion coefficients of DiMFc and $DiMFc^+$ in W are also assumed to be 9.6×10^{-6} $cm^2\ s^{-1}$, on the assumption that $D^W/D^{DCE} = 0.875$ (being approximated to the reciprocal ratio of the viscosities of W and DCE, i.e., 0.890 and 0.779 mPa s,[45] respectively, at 25 °C). For the diffusion coefficient of Cyt *c* (in either the oxidized or reduced form) in W, a literature value[44] of 1.28×10^{-6} $cm^2\ s^{-1}$ has been employed.

Because the interfacial IT is generally very fast, the IT of $DiMFc^+$ (=O2) is assumed to obey the Nernst equation

$$\Delta_O^W\phi = \Delta_O^W\phi_{IT}^{o} + \frac{RT}{F}\ln\left(\frac{\gamma_{O2}^O}{\gamma_{O2}^W}\right) + \frac{RT}{F}\ln\left(\frac{[O2]_O}{[O2]_W}\right) = \Delta_O^W\phi_{IT}^{o'} + \frac{RT}{F}\ln\left(\frac{[O2]_O}{[O2]_W}\right) \tag{6}$$

where $\Delta_O^W\phi_{IT}^{o'}$ is the formal IT potential of $DiMFc^+$ at the DCE/W interface, which has been estimated to be −0.033 V from a separate CV measurement[46] (note that in the curve fitting analyses described below $\Delta_O^W\phi_{IT}^{o'}$ has been employed as an adjusting parameter for obtaining better fitting results). Also note that $[O2]_O$ and $[O2]_W$ in eq 6 correspond to the values just at the O/W interface.

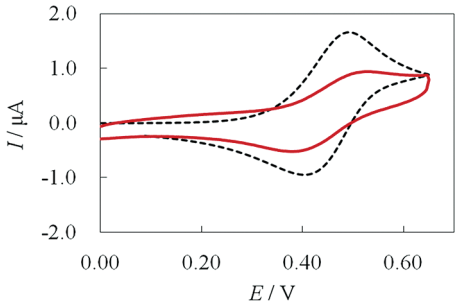

Figure 4. Cyclic voltammogram observed with the ECSOW system in the presence of 0.4 mM Cyt *c* in W (containing 0.1 M $NaClO_4$ + 10 mM 4,4′-bipyridine; pH 6.9) and 0.02 M DiMFc in DCE (containing 0.02 M BTPPATClPB). In the respective phases, Au and Pt disk electrodes connected with an electric wire were immersed. The dashed curve represents the simulated voltammogram obtained for the reversible ET between Cyt *c* and DiMFc via the EC phase with $\Delta_O^W\phi_{ET}^{o'} = 0.259$ V. Scan rate: 50 mV s^{-1}.

In the proposed mechanism, the kinetically controlled process is the homogeneous ET between DiMFc and Cyt c_{OX} in the W phase (eq 4b). The reaction rate v_{hom} is expressed as

$$v_{hom} = -\frac{d[R2]_W}{dt} = \frac{d[O2]_W}{dt} = -\frac{d[O1]_W}{dt} = \frac{d[R1]_W}{dt} = k_1[R2]_W[O1]_W - k_2[O2]_W[R1]_W \tag{7}$$

where O1 = Cyt c_{OX}, R1 = Cyt c_{RED}, O2 = $DiMFc^+$, and R2 = DiMFc; and k_1 and k_2 are the forward and backward second-order rate constants, respectively. In equilibrium (i.e., $v_{hom} = 0$), we obtain

$$\frac{[R1]_W[O2]_W}{[O1]_W[R2]_W} = \frac{k_1}{k_2} = K_{hom} \tag{8}$$

When the overall ET reaction across the O/W interface is in equilibrium, the following equation should be valid for the interfacial concentrations, regardless of the reaction mechanism adopted.

$$\Delta_O^W\phi = \Delta_O^W\phi_{ET}^{o'} + \frac{RT}{F}\ln\left(\frac{[R1]_W[O2]_O}{[O1]_W[R2]_O}\right) \tag{9}$$

Here, $\Delta_O^W\phi_{ET}^{o'}$ ($=E_{ET}^{o'} - \Delta E_{ref}$) is the formal potential for the overall ET reaction:

$$\Delta_O^W\phi_{ET}^{o'} = E_{O2/R2}^{o'} - E_{O1/R1}^{o'} \tag{10}$$

where $E_{O2/R2}^{o'}$ and $E_{O1/R1}^{o'}$ are the formal potentials of the redox couples in the respective phases, which are expressed on the same potential scale. In this study the value of $\Delta_O^W\phi_{ET}^{o'}$ has been obtained from a voltammetric measurement with the ECSOW system. Figure 4 shows the cyclic voltammogram for the ECSOW system in the presence of 0.4 mM Cyt *c* in W and 0.02 M DiMFc in DCE. A clear quasi-reversible wave is observed for the ET between Cyt *c* and DiMFc via the EC phase. As shown by the dashed line in Figure 4, the observed wave (solid line) can be reproduced at the same potential by digital simulation assuming a

dx.doi.org/10.1021/jp2092658 |J. Phys. Chem. B 2012, 116, 585–592

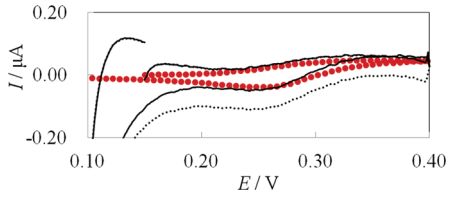

Figure 5. Curve fitting of the cyclic voltammogram obtained using the electrochemical cell (Scheme 1) with $x = 0.4$ and $y = 0.02$. The solid line shows the experimental voltammogram corrected for the base current obtained in the absence of Cyt *c*, though the current on the reverse (cathodic) scan was shifted up by 0.07 μA so that there was no current drop at the switching potential. The solid circles show the theoretical voltammogram obtained by assuming the IT mechanism in Figure 3. The adjusting parameters: $k_1 = 7 \times 10^6\ M^{-1}\ s^{-1}$ and $\Delta_O^W\phi_{IT}^{o'} = -0.047$ V. Scan rate: 50 mV s^{-1}.

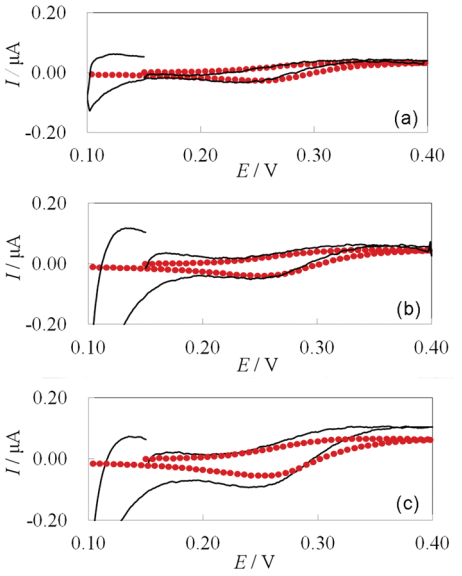

Figure 6. Comparison of the experimental (solid line) and theoretical (solid circles) cyclic voltammograms obtained using the electrochemical cell (Scheme 1) with x = (a) 0.2, (b) 0.4, and (c) 0.8 and $y = 0.02$. Each experimental current on the reverse scan was corrected in the same manner as in Figure 5. The theoretical current was calculated with $k_1 = 7 \times 10^6\ M^{-1}\ s^{-1}$ and $\Delta_O^W\phi_{IT}^{o'} = -0.047$ V. Scan rate: 50 mV s^{-1}.

reversible ET via the EC phase. However, the observed current is small rather than the theoretical one. This is probably because of a kinetic effect and a possible lower electrolysis efficiency of Cyt *c* at the Au electrode, though the convincing reason needs further research. Nevertheless, the value of $\Delta_O^W\phi_{ET}^{o'}$ can be determined to be 0.259 V. On the other hand, the $\Delta_O^W\phi_{ET}^{o'}$ value has been estimated to be 0.238 V from the literature values of $E_{O2/R2}^{o'} = 0.495$ V[47] and $E_{O1/R1}^{o'} = 0.257$ V[2] (at pH 7) both vs SHE. The estimated $\Delta_O^W\phi_{ET}^{o'}$ value is in reasonable agreement with the value of 0.259 V *directly* determined with the ECSOW system.

From eqs 6, 8, and 9, the following relation can be obtained

$$K_D \exp\left[\frac{F}{RT}(\Delta_O^W\phi_{IT}^{o\prime} - \Delta_O^W\phi_{ET}^{o\prime})\right] = K_{hom} = \frac{k_1}{k_2} \qquad (11)$$

Thus, the value of K_{hom} is determined from the values of K_D, $\Delta_O^W\phi_{IT}^{o'}$, and $\Delta_O^W\phi_{ET}^{o'}$. Then the value of k_2 corresponding to an arbitrary value of k_1 is obtained from the K_{hom} value. In the present curve fitting analysis with $K_D = 6800$ and $\Delta_O^W\phi_{ET}^{o'} = 0.259$ V, $\Delta_O^W\phi_{IT}^{o'}$ and k_1 have been used as the adjusting parameters.

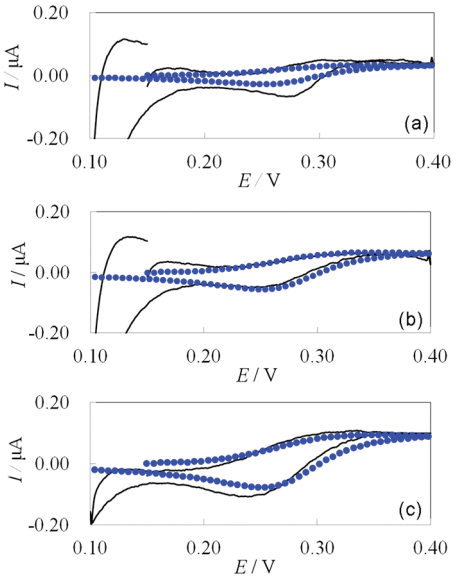

Figure 7. Comparison of the experimental (solid line) and theoretical (solid circles) cyclic voltammograms obtained using the electrochemical cell (Scheme 1) with $x = 0.4$ and y = (a) 0.01, (b) 0.02, and (c) 0.04. Each experimental current on the reverse scan was corrected in the same manner as in Figure 5. The theoretical current was calculated with $k_1 = 7 \times 10^6\ M^{-1}\ s^{-1}$ and $\Delta_O^W\phi_{IT}^{o'} = -0.047$ V. Scan rate: 50 mV s^{-1}.

In Figure 5, the solid line shows an experimental cyclic voltammogram corrected for the base current obtained in the absence of Cyt *c*. In practice, however, at the switching potential at 0.40 V, the current dropped down as shown by the dotted line. This current drop appeared to be due to the change of C_{dl} with the adsorption of Cyt *c* at the O/W interface (see below). Accordingly, the current on the reverse scan was shifted up by 0.07 μA so that there was no current drop at the switching potential. The thus-corrected current was then used for the curve fitting by digital simulation. As shown by the solid circles in Figure 5, the experimental voltammogram has been well reproduced by using the IT mechanism. One of the two adjusting parameters, k_1, is $7 \times 10^6\ M^{-1}\ s^{-1}$, being comparable with the second-order rate constant ($12 \times 10^6\ M^{-1}\ s^{-1}$) for the ET between Cyt *c* and $Fe(CN)_6^{3-}$.[48] The other adjusting parameter, $\Delta_O^W\phi_{IT}^{o'}$, is −0.047 V, being in reasonable agreement with the value of −0.033 V determined by a separate experiment.[46] Using these parameters, we simulated cyclic voltammograms obtained for a variety of other concentration conditions.

A comparison is made between the experimental cyclic voltammograms (Figure 6) obtained for three different concentrations of Cyt *c* and their theoretical values. The result shown in Figure 6b is the same as in Figure 5. As shown in Figures 6a and 6c, the voltammograms obtained for different Cyt *c* concentrations are well reproduced with the same parameter set (i.e., $k_1 = 7 \times 10^6\ M^{-1}\ s^{-1}$ and $\Delta_O^W\phi_{IT}^{o'} = -0.047$ V). Likewise, as shown in Figure 7, the voltammograms obtained for different DiMFc concentrations could be reproduced satisfactorily. Furthermore, though the data are not shown, the dependence of the voltammograms on the voltage scan rate is reproduced in the same manner. These results clearly suggest the validity of the IT mechanism.

dx.doi.org/10.1021/jp2092658 |*J. Phys. Chem. B* 2012, 116, 585–592

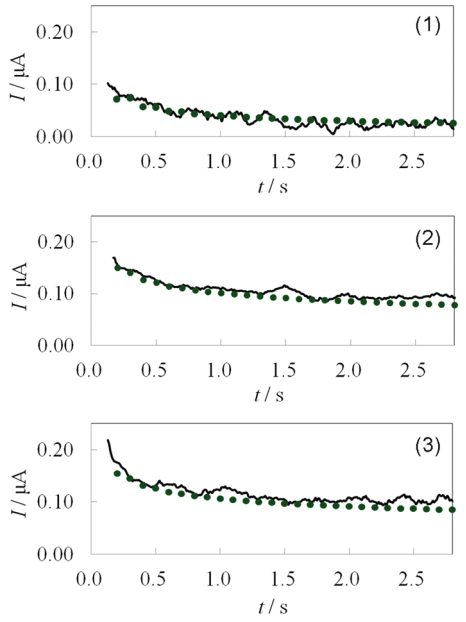

Figure 8. Curve fitting of the baseline-corrected potential-step chronoamperograms obtained using the electrochemical cell (Scheme 1) with $x = 0.4$ and $y = 0.02$. The applied potential: (1) 0.310, (2) 0.360, and (3) 0.420 V (with the initial potential set at 0.150 V). The solid circles show the theoretical chronoamperograms obtained by assuming the IT mechanism in Figure 3. The adjusting parameters: $k_1 = 7 \times 10^6\ M^{-1}\ s^{-1}$ and $\Delta_O^W\phi_{IT}^{o'} = -0.011$ V.

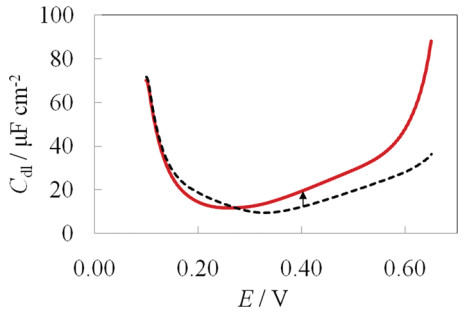

Figure 9. Double-layer capacity of the DCE/W interface in the absence (dashed line) and presence (solid line) of 0.4 mM Cyt *c* in the W phase (pH 6.9).

Digital Simulation in PSCA. Furthermore, we performed curve fitting of potential-step chronoamperograms. In Figure 8, the solid lines show the chronoamperograms, i.e., current−time curves obtained for three different applied potentials, i.e., 0.310, 0.360, and 0.420 V (with the initial potential set at 0.150 V). In a similar manner as in CV, the IT mechanism (Figure 3) is assumed in the curve fitting analysis. As shown by the solid circles, the theoretical current values are well fitted to the experimental ones in the time range of 0.15−2.8 s. The values of k_1 and $\Delta_O^W\phi_{IT}^{o'}$ are then obtained as the adjusting parameters: $k_1 = 7 \times 10^6\ M^{-1}\ s^{-1}$ and $\Delta_O^W\phi_{IT}^{o'} = -0.011$ V. The k_1 value is equal to that obtained for the curve fitting in CV. The $\Delta_O^W\phi_{IT}^{o'}$ value is in reasonable agreement with the value of −0.033 V determined by the separate experiment.[46] Thus, the validity of the IT mechanism has been further confirmed.

Interfacial Adsorption of Cyt *c*. According to the IT mechanism, the ET between DiMFc and Cyt *c* occurs not at the O/W interface but in the W phase. However, it should be noted that Cyt *c* is adsorbed at the DCE/W interface. Figure 9 shows the double-layer capacity (C_{dl}) of the DCE/W interface in the presence and absence of Cyt *c* in W. As is seen in the figure, the capacity curve is shifted to lower potentials in the presence of Cyt *c*. This may be elucidated in terms of the interfacial adsorption of Cyt *c* molecules having a positive charge[49] (+9.2) at pH 6.9. It is considered that the capacity minimum potential close to the point of zero charge (pzc) is affected by the positive fixed charge due to the adsorbed proteins. We would like to add that the current drop observed at 0.4 V in CV (Figure 5) corresponds well to the increase of C_{dl} at the potential (see the arrow in Figure 9).

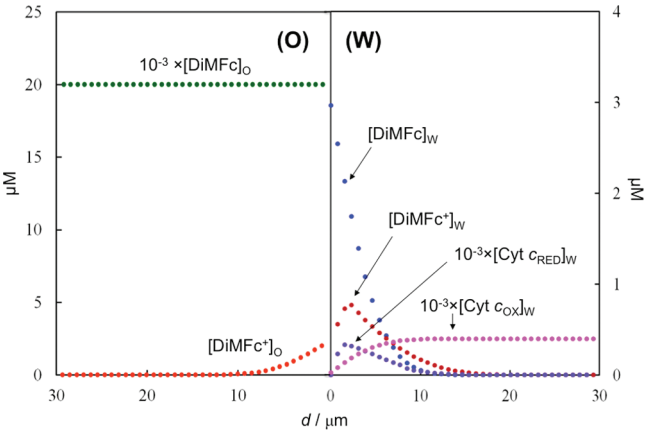

Figure 10. Snapshot of the concentration profiles of DiMFc, DiMFc$^+$, Cyt c_{OX}, and Cyt c_{RED}, obtained by the digital simulation, at $E = 0.400$ V (i.e., 5 s after a voltammetric sweep at 50 mV s^{-1}). Initial conditions are as in Figure 5. As indicated, some concentration values are multiplied by 10^{-3}. Note that $[DiMFc]_O$ at any distance (d) from the interface is assumed to be equal to the bulk concentration. It is also assumed that $[DiMFc]_W$ is constant at $d = 0$ (see eq 5).

It has thus been confirmed that Cyt *c* is adsorbed at the DCE/W interface. Nevertheless, as shown by the above digital simulation results, the ET reaction between Cyt *c* and DiMFc at the interface could be explained without considering any contribution from the proteins existing on the interface. One of the reasons might be the denaturation or unfolding of Cyt *c* molecules at the O/W interface. Recently, the denaturation of hemoglobin at the O/W interface has been investigated by means of CV.[50] It has been described that the denatured protein is less electroactive at the O/W interface.

However, an additional, and probably principal reason is the large thickness of the "reaction layer" formed on the W-phase side of the interface (Figure 3). The reaction-layer thickness (μ) is given by[51]

$$\mu = \sqrt{\frac{D_{Cyt\ c}}{k_1[DiMFc]_W}} \qquad (12)$$

with $[DiMFc]_W = [DiMFc]_O/K_D$. Using the values of $D_{Cyt\ c} = 1.28 \times 10^{-6}\ cm^2\ s^{-1}$,[44] $k_1 = 7 \times 10^6\ M^{-1}\ s^{-1}$, and $K_D = 6800$, μ is then estimated to be ~2.5 μm for a typical case, i.e., $[DiMFc]_O = 0.02$ M. The reaction layer can also be confirmed by the concentration profiles of the redox species, obtained by the digital simulation. It is seen in Figure 10 that the homogeneous ET reaction in W occurs predominantly in a layer of several micrometers

dx.doi.org/10.1021/jp2092658 |*J. Phys. Chem. B* 2012, 116, 585–592

adjacent to the interface. This thickness of the layer is much larger than the size of a Cyt *c* molecule (the radius estimated from the molecular volume[52] is 1.44 nm). Accordingly, the amount of Cyt *c* present in the reaction layer would be much larger than that on the O/W interface. For this reason, the contribution from Cyt *c* adsorbed at the interface, if any, should be considered as negligible.

CONCLUDING REMARKS

Cyt *c* undergoes ET with DiMFc not at the DCE/W interface but in the W phase in the vicinity of the interface, even though the partition coefficient of DiMFc is as large as 6800. This is because of the difference in the volume of the reaction field between the heterogeneous and homogeneous ET mechanisms.[15] In the former, the reaction field should be restricted to an interfacial layer as thin as several angstroms, whereas in the latter, the reaction-layer thickness is in the micrometer range as described above. Therefore, the volume of the reaction field for the homogeneous ET (i.e., the IT mechanism) would be $\sim 10^4$ times larger than that for the heterogeneous ET. This leads to an advantage of the IT mechanism, which would overcome its disadvantage, i.e., the small partition of DiMFc into W (cf. K_D = 6800). However, if a more extremely hydrophobic electron donor would be used instead of DiMFc, there would be a possibility for heterogeneous ET at the O/W interface. In any case, the present study shows that the ET of Cyt *c* at the O/W interface is mainly driven in the bulk W phase nearest the interface. This would be highly suggestive when considering the behaviors of Cyt *c* in the mitochondrial respiratory chain.[1] It seems commonly believed that Cyt *c* undergoes ET in the aquatic environment, i.e., in the thyrakoid intermembrane space. The present study may suggest that the membrane potential does not directly affect the ET steps of Cyt *c* with complexes III and IV.

AUTHOR INFORMATION

Corresponding Author

*E-mail: osakai@kobe-u.ac.jp.

Present Addresses

[†]Analysis Technology Research Center, Sumitomo Electric Industries Ltd., 1−1−3 Shimaya, Konohana-ku, Osaka 554−0024, Japan.

REFERENCES

(1) Berg, J. M.; Tymoszko, J. L.; Stryer, L. *Biochemistry*; W. H. Freeman and Co.: New York, 2010; Chapter 18.
(2) Yeh, P.; Kuwana, T. *Chem. Lett.* **1977**, 1145–1148.
(3) Shibata, M.; Furuya, N. *J. Electroanal. Chem.* **1988**, *250*, 201–206.
(4) Wang, L.; Wang, E. *Electrochem. Commun.* **2004**, *6*, 49–54.
(5) Davis, J. J.; Coles, R. J.; Allen, H.; Hill, O. *J. Electroanal. Chem.* **1997**, *440*, 279–282.
(6) Wang, J.; Li, M.; Shi, Z.; Li, N.; Gu, Z. *Anal. Chem.* **2002**, *74*, 1993–1997.
(7) Alwarappan, S.; Joshi, R. K.; Ram, M. K.; Kumar, A. *Appl. Phys. Lett.* **2010**, *96*, 263702.
(8) Armstrong, F. A.; Bond, A. M.; Hill, H. A. O.; Oliver, B. N.; Psalti, I. S. M. *J. Am. Chem. Soc.* **1989**, *111*, 9185–9189.
(9) *Liquid Interfaces in Chemical, Biological, and Pharmaceutical Applications*; Volkov, A. G., Ed.; Marcel Dekker: New York, 2001.
(10) *The Interface Structure and Electrochemical Processes at the Boundary between Two Immiscible Liquids*; Kazarinov, V. E., Ed.; Springer-Verlag: Berlin, 1987.
(11) *Liquid-Liquid Interfaces, Theory and Methods*; Volkov, A. G., Deamer, D. W., Eds.; CRC press: Boca Raton, FL, 1996.
(12) Girault, H. H.; Schiffrin, D. J. In *Electroanalytical Chemistry*; Bard, A. J., Ed.; Marcel Dekker: New York, 1989; Vol. 15, p 1−141.
(13) Senda, M.; Kakiuchi, T.; Osakai, T. *Electrochim. Acta* **1991**, *36*, 253–262.
(14) Samec, Z. *Pure Appl. Chem.* **2004**, *76*, 2147–2180.
(15) Osakai, T.; Hotta, H. In *Interfacial Nanochemistry*; Watarai, H., Teramae, N., Sawada, T., Eds.; Kluwer Academic/Plenum Publishers: New York, 2005; Chapter 8.
(16) Samec, Z.; Mareček, V.; Weber, J. *J. Electroanal. Chem.* **1979**, *103*, 11–18.
(17) Hotta, H.; Ichikawa, S.; Sugihara, T.; Osakai, T. *J. Phys. Chem. B* **2003**, *107*, 9717–9725.
(18) Tatsumi, H.; Katano, H. *Anal. Sci.* **2004**, *20*, 1613–1615.
(19) Tatsumi, H.; Katano, H. *J. Electroanal. Chem.* **2006**, *592*, 121–125.
(20) Tatsumi, H. *Rev. Polarogr.* **2008**, *54*, 89–97.
(21) Osakai, T.; Akagi, N.; Hotta, H.; Ding, J.; Sawada, S. *J. Electroanal. Chem.* **2000**, *490*, 85–92.
(22) Osakai, T.; Jensen, H.; Nagatani, H.; Fermín, D. J.; Girault, H. H. *J. Electroanal. Chem.* **2001**, *510*, 43–49.
(23) Sugihara, T.; Hotta, H.; Osakai, T. *Bunseki Kagaku* **2003**, *52*, 665–671.
(24) Geblewicz, G.; Schiffrin, D. J. *J. Electroanal. Chem.* **1988**, *244*, 27–37.
(25) Cunnane, V. J.; Schiffrin, D. J.; Beltran, C.; Geblewicz, G.; Solomon, T. *J. Electroanal. Chem.* **1988**, *247*, 203–214.
(26) Osakai, T.; Ichikawa, S.; Hotta, H.; Nagatani, H. *Anal. Sci.* **2004**, *20*, 1567–1573.
(27) Osakai, T.; Okamoto, M.; Sugihara, T.; Nakatani, K. *J. Electroanal. Chem.* **2009**, *628*, 27–34.
(28) Georganopoulou, D. G.; Caruana, D. J.; Strutwolf, J.; Williams, D. E. *Faraday Discuss.* **2000**, *116*, 109–118.
(29) Sugihara, T.; Hotta, H.; Osakai, T. *Phys. Chem. Chem. Phys.* **2004**, *6*, 3563–3568.
(30) Sasaki, Y.; Sugihara, T.; Osakai, T. *Anal. Biochem.* **2011**, *417*, 129–135.
(31) Lillie, G. C.; Holmes, S. M.; Dryfe, R. A. W. *J. Phys. Chem. B* **2002**, *106*, 12101–12103.
(32) The fraction of the oxidized form was roughly estimated to be ∼91% from the molar adsorption coefficient at 550 nm. Van Gelder, B. F.; Slater, E. C. *Biochim. Biophys. Acta* **1962**, *58*, 593–595.
(33) Osakai, T.; Yamada, H.; Nagatani, H.; Sagara, T. *J. Phys. Chem. C* **2007**, *111*, 9480–9487.
(34) Aoyagi, S.; Matsudaira, M.; Suzuki, T.; Katano, H.; Sawada, S.; Hotta, H.; Ichikawa, S.; Sugihara, T.; Osakai, T. *Electrochemistry* **2002**, *70*, 329–333.
(35) Wandlowski, T.; Mareček, V.; Samec, Z. *Electrochim. Acta* **1990**, *35*, 1173–1175.
(36) Osakai, T.; Kakutani, T.; Senda, M. *Bull. Chem. Soc. Jpn.* **1983**, *56*, 991–996.
(37) Hotta, H.; Akagi, N.; Sugihara, T.; Ichikawa, S.; Osakai, T. *Electrochem. Commun.* **2002**, *4*, 472–477.
(38) Eddowes, M. J.; Hill, H. A. O. *J. Am. Chem. Soc.* **1979**, *101*, 4461–4464.
(39) Feldberg, S. W. In *Electroanalytical Chemistry*; Bard, A. J., Ed.; Marcel Dekker: New York, 1969; Vol. 3, pp 199−296.
(40) Bard, A. J.; Faulkner, L. R. *Electrochemical Methods, Fundamentals and Applications*, 2nd ed; Wiley: New York, 2001; pp 785−807.
(41) Feldberg, S. W. *J. Electroanal. Chem.* **1981**, *127*, 1–10.
(42) Shinshi, M.; Sugihara, T.; Osakai, T.; Goto, M. *Langmuir* **2006**, *22*, 5937–5944.
(43) Kakutani, T.; Osakai, T.; Senda, M. *Bull. Chem. Soc. Jpn.* **1983**, *56*, 991–996.
(44) Sivakolundu, S. G.; Mabrouk, P. A. *J. Am. Chem. Soc.* **2000**, *122*, 1513–1521.
(45) *CRC Handbook of Chemistry and Physics*, 82nd ed.; Lide, D. R., Ed.; CRC Press: Boca Raton, FL, 2001.

(46) In the same cell system as in Scheme 1, a reversible wave for the transfer of $DiMFc^+$ at the DCE/W interface was obtained by CV with the addition of 0.1 mM $(DiMFc)_3PW_{12}O_{40}$ (prepared according to ref 29) to the DCE phase. From the midpoint potential (+0.270 V) of the reversible wave, the value of $\Delta_O^W\phi_{IT}^{o'}$ was estimated to be −0.033 V.

(47) Langmaier, J.; Trojánek, A.; Samec, Z. *J. Electroanal. Chem.* **2008**, *616*, 57–63.

(48) Butler, J.; Chapman, S. K.; Davies, D. M.; Sykes, A. G.; Speck, S. H.; Osheroff, N.; Margoliash, E. *J. Biol. Chem.* **1983**, *258*, 6400–6404.

(49) Simply estimated from the amino acid sequence of Cyt *c* (from horse heart), which is available in the Protein Data Bank Japan (http://www.pdbj.org/index_j.html).

(50) Herzog, G.; Eichelmann-Daly, P.; Arrigan, D. W. M. *Electrochem. Commun.* **2010**, *12*, 335–337.

(51) Senda, M. *Rev. Polarogr.* **2003**, *49*, 219–228. Corrections *Rev. Polarogr.* **2004**, *50*, 60–61.

(52) Chalikian, T. V.; Totrov, M.; Abagyan, R.; Breslauer, K. J. *J. Mol. Biol.* **1996**, *260*, 588–603.